42 *Biochemistry* **2010,** *49,* 42–48
DOI: 10.1021/bi901484b

BIOCHEMISTRY
including biophysical chemistry & molecular biology
Article

Role of a Highly Conserved Electrostatic Interaction on the Surface of Cytochrome *c* in Control of the Redox Function[†]

Hulin Tai, Shin-ichi Mikami, Kiyofumi Irie, Naoki Watanabe, Naoya Shinohara, and Yasuhiko Yamamoto*

Department of Chemistry, University of Tsukuba, Tsukuba 305-8571, Japan

Received August 25, 2009; Revised Manuscript Received November 25, 2009

ABSTRACT: In *Hydrogenobacter thermophilus* cytochrome c_{552}, an electrostatic interaction between Lys8 and Glu68 in the N- and C-terminal helices, respectively, stabilizes its protein structure [Travaglini-Allocatelli, C., Gianni, S., Dubey, V. K., Borgia, A., Di Matteo, A., Bonivento, D., Cutruzzola, F., Bren, K. L., and Brunori, M. (2005) *J. Biol. Chem. 280*, 25729−25734], this electrostatic interaction being a highly conserved structural feature of the cytochrome *c* family. In the present study, the functional consequences of removal of the interaction through replacement of Lys8 by Ala have been investigated in order to elucidate the molecular mechanisms responsible for functional control of the protein. The mutation resulted in a decrease in protein stability, as reflected in lowering of the denaturation temperature by ∼2−9 °C, and a negative shift by ∼8 mV of the redox potential (E_m) of the protein. The decrease in the protein stability was attributed to the enthalpic loss due to the removal of the intramolecular interaction. The negative shift of the E_m value was shown to be due to the effect of the mutation on the entropic contribution to the E_m value. The small, but subtle, effects of removal of the conserved electrostatic interaction, occurring at ∼1.4 nm away from heme iron, on the thermodynamic properties of the protein demonstrated not only that the interaction is important for maintaining the functional properties of the protein but also that amino acid residues relatively remote from the heme active site play sizable roles in functional control of the protein.

The protein matrix significantly modifies the electrochemistry of the heme in cytochromes. Within the framework of the monoheme class I cytochrome *c* (cyt *c*)[1] structure, the redox potential (E_m) varies by more than 800 mV (*1*). Understanding how a protein modifies the E_m value of the heme should lead to a general description of the relationship between the structures and functions of biopolymers (*1*−*8*). We have been investigating the molecular mechanisms responsible for control of the E_m values of cyts *c* through a comparative study on homologous *Hydrogenobacter thermophilus* cytochrome c_{552} (HT) (*9*) and *Pseudomonas aeruginosa* cytochrome c_{551} (PA) (*10*). HT and PA exhibit 56% sequence homology with each other and hence almost identical protein folding. Despite their structural similarity, there is a remarkable difference not only in the E_m value but also in the denaturation temperature (T_m) between the two proteins (*11*−*17*). We have revealed that the E_m value of a protein is controlled primarily through the thermodynamic stability of the oxidized form of the protein, which has been shown to depend upon structural properties of the protein interior such as the Fe−Met coordination bond strength and the ionization state of the buried heme 17-propionic acid side chain (*15*−*18*). These findings have been successfully utilized for tuning of the E_m value of a protein over the range up to 300 mV (*15*, *17*, *19*).

In general, packing of the hydrophobic core, disulfide and salt bridges, hydrogen bonding, and intrinsic secondary structure propensities have been shown to stabilize the protein structure (*20*). In the case of cyts *c*, it has been shown that, upon reinforcement of the hydrophobic protein interior through reduction of the void space by means of amino acid replacements, an oxidized protein is more significantly stabilized than its reduced form, leading to a decrease in difference in the thermodynamic stability between the two redox forms of the protein, which in turn results in a negative shift of the E_m value relative to that of the wild-type protein (*15*, *17*, *21*). For example, removal of a single hydroxyl group from the hydrophobic core of HT, through replacement of a Tyr by a Phe (Y25F mutation), resulted in elevation of the T_m value of the oxidized form by ∼6 °C, the T_m value of the reduced form remaining essentially unaltered (*21*). As a result, the E_m value of Y25F showing higher stability in the oxidized form exhibited a negative shift of ∼20 mV relative to that of the wild-type HT in an enthalpic manner (*21*). Thus, there is a close relationship between the stability and redox function of cyts *c*.

In this study, we investigated the role of a highly conserved electrostatic interaction on the surface of cyts *c* in the control of protein stability and redox function. According to the X-ray structure of HT, the side chain of Lys8 located in the last turn of the N-terminal helix interacts electrostatically with that of Glu68 located in the first turn of the C-terminal helix and also possibly forms a hydrogen bond with the main chain carbonyl oxygen of

[†]This work was supported by MEXT, the Yazaki Memorial Foundation for Science and Technology, and the NOVARTIS Foundation (Japan) for the Promotion of Science.

*Corresponding author. Phone and Fax: +81-29-853-6521. E-mail: yamamoto@chem.tsukuba.ac.jp.

[1]Abbreviations: cyts *c*, cytochromes *c*; E_m, redox potential; HT, *Hydrogenobacter thermophilus* cytochrome c_{552}; PA, *Pseudomonas aeruginosa* cytochrome c_{551}; T_m, denaturation temperature; CV, cyclic voltammetry; HSQC, heteronuclear single-quantum correlation spectroscopy, E_m−T plots, plots of redox potentials of proteins against temperature.

 Published on Web 12/01/2009

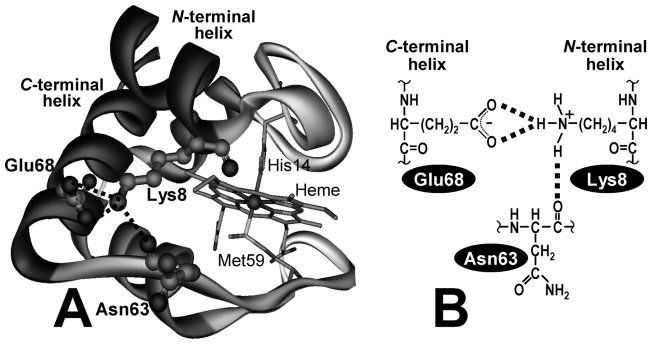

FIGURE 1: (A) Schematic representation of the structure of *H. thermophilus* cytochrome c_{552} (HT) (*9*) and locations of amino acid residues Lys8, Asn63, and Glu68. The polypeptide chain is illustrated as a ribbon model and the heme, together with Fe-coordinated His14 and Met59, is drawn as a stick model. Lys8, Asn63, and Glu68 are shown as a ball and stick model, and the interactions among the residues are illustrated by a gray broken line. (B) Schematic drawing of the electrostatic interaction between the side chains of Lys8 and Glu68 and the hydrogen bond between the side chain of Lys8 and the main chain of Asn63. The interactions are represented by bold broken lines.

Asn63 located in the loop region bearing axial Met59 coordinated to heme iron (*9*) (Figure 1). This electrostatic interaction between residues in the two helices at opposite ends of the polypeptide chain is a highly conserved structural feature of the cyt *c* family and has been shown to contribute to stabilization of the pairing of the two helices (*2*, *22*). Such a bihelical association has been shown to be critical for initiation of the protein folding and hence plays a crucial role in determining the pathway and kinetics of the folding/unfolding of the protein (*22*). In order to determine the roles of the electrostatic interaction between Lys8 and Glu68 (Lys8/Glu68 interaction) in the control of the stability and redox function of the protein, we have abolished both the Lys8/Glu68 interaction and the hydrogen bond between Lys8 and Asn63 by replacement of Lys8 by an Ala (K8A mutation). The K8A mutation should lead to a decrease in the stability of the bihelical association, which is expected to result in a decrease in the stability of the overall protein structure. The K8A mutant has been subjected to a detailed study on the structure−function relationship involving paramagnetic NMR and circular dichroism (CD) measurements in the temperature range of 30−155 °C (*16*) and cyclic voltammetry (CV) in order to determine the effect of removal of the Lys8/Glu68 interaction on the functional properties of the protein. In addition, double mutant K8A/Y25F has been similarly characterized to elucidate the relationship between the effects of the K8A and Y25F mutations on the stability and redox function of the protein. The study demonstrated that the stabilities of the oxidized and reduced proteins are decreased by the K8A mutation, confirming that the Lys8/Glu68 interaction contributes to the overall protein stabilities of both the oxidized and reduced forms of the protein. The E_m value of the K8A mutant at pH 6.0 and 25 °C was 236.9 mV, this being lower by ~8 mV relative to that of the wild-type HT. Determination of the E_m values of the K8A mutant and wild-type HT revealed that both the enthalpic (ΔH) and entropic (ΔS) contributions to the E_m value were appreciably affected by the K8A mutation, despite the fact that the electrostatic interaction occurs at ~1.4 nm away from the heme iron. This result was a sharp contrast to the case of the Y25F mutation, where only the ΔH value was affected by the mutation (*21*). In addition, studies on the K8A/Y25F mutant demonstrated that the effects of the K8A and Y25F mutations on the protein stability and redox function are almost independent of each other. These findings provide novel insights as to tuning of the stability and redox function of cyts *c* through protein engineering.

MATERIALS AND METHODS

Protein Samples. The wild-type HT and its mutants were produced using *Escherichia coli* and purified as reported previously (*11*, *12*). The oxidized forms of the proteins were prepared by the addition of a 10-fold molar excess of potassium ferricyanide. For NMR samples, the proteins were concentrated to about 1 mM in an ultrafiltration cell (YM-5; Amicon), and then 10% ^2H_2O was added to the protein solutions. The pH of each sample was adjusted using 0.2 M KOH or 0.2 M HCl, and the pH was monitored with a Horiba F-22 pH meter with a Horiba type 6069-10C electrode.

^1H NMR. NMR spectra were recorded on a Bruker Avance 600 FT NMR spectrometer operating at the ^1H frequency of 600 MHz. Samples for NMR measurements comprised ~1.0 mM protein in nominal ^1H_2O (~90% ^1H_2O/~10% ^2H_2O), together with 20 mM potassium phosphate buffer, pH 7.0. Typical spectra of reduced cyts *c* required a 15 kHz spectral width, 32K data points, an ~10 μs 90° pulse, an ~1.5 s recycle time, and ~1K scans, and the water signal was eliminated using water suppression by means of gradient-tailored excitation (WATERGATE) (*23*). On the other hand, typical spectra of oxidized cyts *c* required a 100 kHz spectral width, 32K data points, an ~10 μs 90° pulse, an ~1 s recycle time, and 2K scans, and the water signal was suppressed with a 100 ms presaturation pulse. Chemical shifts are given in parts per million downfield from sodium 2,2-dimethyl-2-silapentane-5-sulfonate with H_2O as an internal reference.

CD Spectroscopy. CD spectra were recorded on a JASCO J-820 spectrometer over the spectral range of 200−250 nm and in the temperature range of 30−155 °C, using an air-tight pressure-proof cell compartment with quartz windows, which was described previously (*16*).

CV. Cyclic voltammograms of the proteins were obtained under a nitrogen atmosphere as described previously (*24*, *25*). A glassy carbon electrode (GCE) was polished with a 0.05 μm alumina slurry and then sonicated in deionized water for 1 min. Two microliters of a 1 mM protein solution was spread evenly with a microsyringe onto the surface of the GCE. Then the GCE surface was covered with a semipermeable membrane. All redox potentials (E_m) were referenced to a standard hydrogen electrode (SHE). The experimental error for E_m was ±2 mV. The variable temperature experiments were performed using a home-built nonisothermal electrochemical cell configuration (*26*, *27*), in which the temperature of the reference electrode was kept constant. The anodic to cathodic peak current ratios obtained at various potential scan rates (1−100 mV s^{-1}) were all ~1. Both the anodic and cathodic peak currents increased linearly as a function of the square root of the scan rate in the range up to 100 mV s^{-1}. Thus, HT and its mutants exhibit quasi-reversible redox processes.

Thermodynamic parameters, i.e., ΔH and ΔS, were calculated from the E_m values attained in the temperature range of ~10 to ~60 °C. The ΔH values were obtained from the slopes of the plots of E_m/T against $1/T$, according to the Gibbs−Helmholtz equation, i.e., $\Delta G = \Delta H - T\Delta S = -nFE_m$. The ΔS values were obtained from the slopes of the plots of E_m against T. The plots

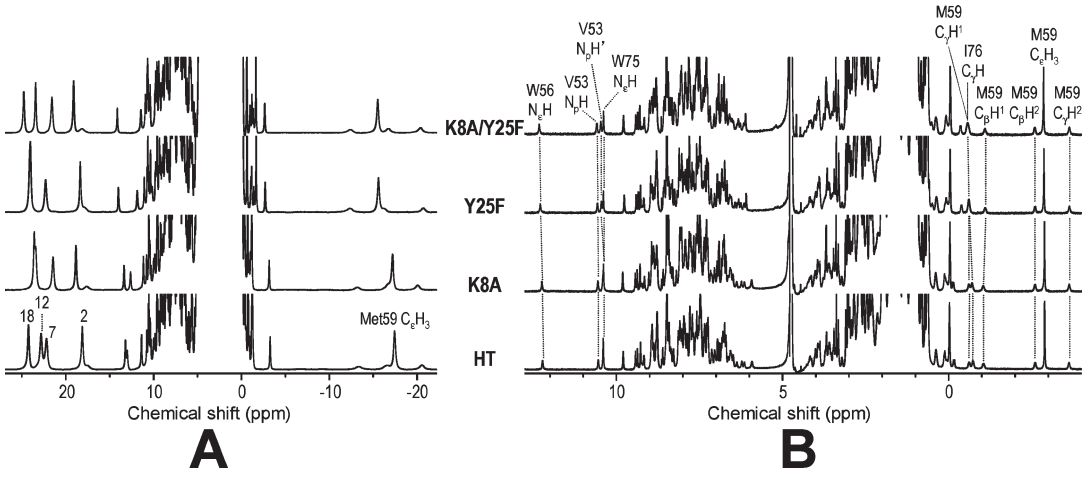

FIGURE 2: 600 MHz ^{1}H NMR spectra of the oxidized (A) and reduced (B) forms of the wild-type HT and K8A, Y25F, and K8A/Y25F mutants in 90% H_2O/10% ^2H_2O, pH 7.0, at 23 °C. Assignments of some signals are indicated with the spectra, and the corresponding resonances are connected by broken lines. The spectra for the wild-type HT and Y25F mutant were reported previously (*21*).

for all the proteins could be fitted by two straight lines with a transition temperature (T_c) of ~35 °C (*25*), and hence two sets of values, ΔH^{low} and ΔS^{low} and ΔH^{high} and ΔS^{high}, in the temperature ranges of $< T_c$ and $> T_c$, respectively, were determined for these proteins. The experimental errors for the ΔH and ΔS values of the proteins were ±2 kJ mol^{-1} and ±3 J K^{-1} mol^{-1}, respectively.

RESULTS

^{1}H NMR Spectra of the K8A and K8A/Y25F Mutants. We first analyzed the effects of the K8A mutation on the heme active site structures of the wild-type HT and Y25F mutant using paramagnetic ^{1}H NMR (Figure 2A). In the ^{1}H NMR spectra of oxidized cyts *c*, paramagnetically shifted heme peripheral side chain methyl and axial Met59 side chain proton signals are resolved in high-frequency- and low-frequency-shifted regions, respectively. These signals have been shown to sensitively reflect structural properties of the heme active site (*28*−*30*). Spectral comparison between the K8A mutant and wild-type HT and the K8A/Y25F and Y25F mutants revealed slight differences in the shifts of the heme methyl and Met59 side chain proton signals. In addition, the shifts of the Met59 side chain proton signals of the reduced forms of the wild-type HT and Y25F mutant were affected very little by the K8A mutation (Figure 2B), indicating that the Met59 side chain conformation is not significantly affected by the mutation. Therefore, the effect of the K8A mutation on the heme methyl proton signals of the oxidized proteins is attributed to alteration of the chemical environment of the heme active site due to the mutation. Since the heme is relatively remote from the K8A mutation site, the alteration of the heme chemical environment caused by the mutation is likely to be a consequence of transmission of the structural perturbation due to the mutation, i.e., the replacement of the Lys side chain by an Ala one and the concomitant loss of the Lys8/Glu68 interaction, to the heme active site through conformational changes of the short loop region containing the so-called heme binding motif, i.e., the amino acid sequence of CxzCH, where amino acid residues are presented as single-letter notations, and x and z represent arbitrary residues, and the long loop bearing the axial Met59 (Figure 1A).

We next investigated the effect of the K8A mutation on protein folding by means of ^{1}H−^{15}N heteronuclear single-quantum correlation spectroscopy (HSQC) (*31*). HSQC cross-peaks have been shown to be highly sensitive to protein folding. Although the cross-peak of the mutated amino acid residue exhibited a change of ~−0.1 ppm only along the ^{1}H axis, those of the other residues of the wild-type HT were essentially unaffected by the mutation (see Supporting Information), indicating that the protein folding is not largely affected by the mutation. The small effect of the K8A mutation on the overall protein folding is consistent with the conclusion, drawn on analysis of the heme and Met59 proton NMR signals of the oxidized protein, that the heme active site structure is essentially unaffected by the K8A mutation.

We have previously shown that neither the heme active site structure nor the protein folding is affected by the Y25F mutation and that the small differences in the shifts between the corresponding proton signals of the oxidized wild-type HT and Y25F mutant are due to alteration of the chemical environment of the heme active site due to removal of the polar OH group of the Tyr25 side chain by the mutation (*21*). Therefore, the differences in the shifts between the corresponding signals of the K8A and K8A/Y25F mutants could also be similarly attributed to the effect of the Y25F mutation on the chemical environment of the heme active site.

Thermostabilities of the K8A and K8A/Y25F Mutants. We next analyzed the thermostabilities of the oxidized and reduced forms of the K8A and K8A/Y25F mutants through measurement of CD spectra (200−250 nm) in the temperature range of 30−155 °C at pH 7.0 (see Supporting Information) (*16*). The fractions of the unfolded proteins calculated from the CD ellipticity at 222 nm were plotted against temperature, thermal unfolding profiles for the two mutants in both redox states being obtained (Figure 3). Similar plots for the wild-type HT and Y25F mutant are also presented, for comparison, in Figure 3. The T_m values of the oxidized and reduced K8A mutant were determined to be 101.1 and 124.1 °C, respectively, and those of the oxidized and reduced K8A/Y25F mutant to be 110.3 and 127.6 °C, respectively (Table 1). The T_m values of these mutants were compared with the values of 109.8 and 129.7 °C for the oxidized and reduced wild-type HT, respectively, and those of 116.1 and 129.7 °C for the oxidized and reduced Y25F mutant, respectively (*21*). The comparison revealed that the K8A mutation significantly decreased the thermostabilities of both the oxidized

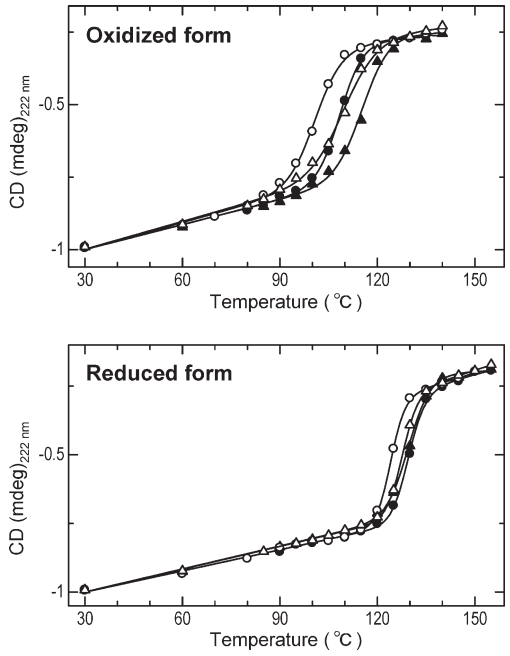

FIGURE 3: Thermal unfolding profiles of the oxidized (top) and reduced (bottom) forms of the wild-type HT (●) and K8A (○), Y25F (▲), and K8A/Y25F (△) mutants at pH 7.0.

Table 1: Denaturation Temperatures and Thermodynamic Parameters of the Redox Reaction for the Wild-Type HT and K8A, Y25F, and K8A/Y25F Mutants

	T_m (°C)[a]			ΔH (kJ mol^{-1})[c]		ΔS (J K^{-1} mol^{-1})[c]	
	oxidized	reduced	E_m (mV)[b]	low	high	low	high
HT	109.8[d]	129.7[d]	245.0	−32.2[e]	−37.5[e]	−28.4[e]	−45.7[e]
K8A	101.1	124.1	236.9	−34.4	−38.2	−38.8	−51.4
Y25F	116.1[e]	129.7[e]	226.7	−31.2[e]	−36.5[e]	−28.5[e]	−44.7[e]
K8A/Y25F	110.3	127.6	219.5	−35.3	−38.5	−47.7	−58.2

[a]Denaturation temperature determined through analysis of the temperature dependence of the CD ellipticity at 222 nm and pH 7.0. The experimental error was ±0.2 °C. [b]Redox potential determined at pH 6.0 and 25 °C. The experimental error was ±2 mV. [c]Entropic and enthalpic contributions to the E_m value at pH 6.0. The experimental errors for ΔH and ΔS of the proteins were ±2 kJ mol^{-1} and ±3 J K^{-1} mol^{-1}, respectively. [d]Cited from ref *16*. [e]Cited from ref *21*. The values had been obtained using the technique described in the present report.

and reduced proteins, indicating that the Lys8/Glu68 interaction contributed to stabilization of the overall protein structure. Furthermore, as in the cases of the HT mutants previously studied (*17*, *21*), for a given protein, the T_m value of the oxidized protein is more significantly decreased by the mutation than that of the reduced one. In addition, since the T_m values of the oxidized forms of all the proteins under consideration are well over 100 °C, the paramagnetically shifted heme methyl and Met59 proton signals could be clearly observed up to 96 °C (see the Supporting Information), reflecting the high thermostabilities of their heme active sites.

E_m Values of the K8A and K8A/Y25F Mutants. We next measured the E_m values of the K8A and K8A/Y25F mutants at 25 °C, the obtained values being compared with those of the wild-type HT and Y25F mutant in Table 1. The E_m values of the K8A and K8A/Y25F mutants were lowered by ∼7 to ∼8 mV relative

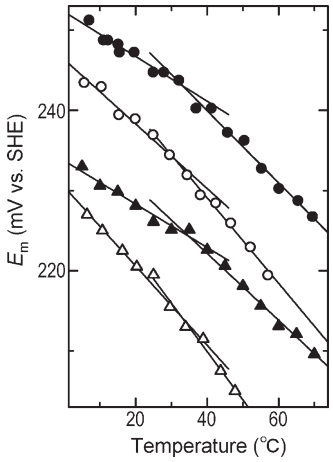

FIGURE 4: Plots of the redox potentials (E_m) against temperature for the wild-type HT (●) and K8A (○), Y25F (▲), and K8A/Y25F (△) mutants at pH 6.0. The plots for the proteins could be fitted by two straight lines with a transition temperature of ∼35 °C, and hence two sets of thermodynamic parameters for the E_m value could be obtained, as shown in Table 1.

to those of the wild-type HT and Y25F mutant, respectively, not only at pH 6.0, but also over the pH range of 5−8 (see Supporting Information). On the other hand, under the experimental conditions used in this study, the E_m value of the Y25F mutant was lower by ∼18 mV relative to that of the wild-type HT, and interestingly, the value of the K8A/Y25F mutant exhibited a similar negative shift, i.e., ∼−17 mV, relative to that of the K8A one. Thus, an additive effect was observed as to the effects of the K8A and Y25F mutations on the E_m values of the proteins.

We also measured the E_m values of the K8A and K8A/Y25F mutants at various temperatures, and the obtained values, together with those of the wild-type HT and Y25F mutant for comparison, are plotted against temperature (E_m-T plots) in Figure 4. From the E_m-T plots, we estimated the ΔH and ΔS contributions to the E_m value (Table 1). The plots for all of the proteins could be fitted by two straight lines with a transition temperature (T_c) of ∼35 °C (*25*) (Figure 4). Hence, two sets of values, ΔH^{low} and ΔS^{low} and ΔH^{high} and ΔS^{high}, in the temperature ranges of $< T_c$ and $> T_c$, respectively, were determined for these proteins (Table 1). The appearance of two different protein structures exhibiting distinctly different thermodynamic parameters has been attributed to a temperature-dependent conformation transition of the heme active site, which is reflected in anomalous line broadening of the paramagnetically shifted heme methyl and Met59 side chain proton signals of the oxidized proteins at lower temperatures (see Supporting Information) (*25*, *32*). Similarly, the heme methyl and Met59 proton signals of the oxidized forms of the K8A and Y25F/K8A mutants at low temperatures also exhibited anomalous line broadening (see Supporting Information).

Comparison of the thermodynamic parameters among the proteins showed that the absolute ΔH^{low}, ΔH^{high}, ΔS^{low}, and ΔS^{high} values ($|\Delta H^{low}|$, $|\Delta H^{high}|$, $|\Delta S^{low}|$, and $|\Delta S^{high}|$, respectively) of the wild-type HT and Y25F mutant were increased by the K8A mutation. We have previously shown that the Y25F mutation of the protein resulted in slight decreases in the $|\Delta H^{low}|$ and $|\Delta H^{high}|$ values, whereas the $|\Delta S^{low}|$ and $|\Delta S^{high}|$ were essentially unaltered (Table 1). Thus, the effects of the K8A and Y25F mutations on the thermodynamic parameters are distinctly different from each other.

DISCUSSION

Effects of the K8A Mutation on Protein Structure and Stability. The NMR studies indicated that the chemical environment of the heme active site was slightly affected by the K8A mutation, whereas the heme active site structure was essentially unaltered. The alteration of the heme chemical environment by the mutation is likely to be due to conformational changes of the loop regions in close proximity to the heme induced by the mutation. This finding indicated that the conserved Lys8/Glu68 interaction contributes to control of the environment of the heme active site in the protein. In addition, analysis of the thermal unfolding profiles of the proteins indicated that the T_m values of both the oxidized and reduced forms of the K8A (or K8A/Y25F) mutant are decreased by ~2 to ~9 °C relative to the corresponding values of the wild-type HT (or Y25F mutant), respectively, confirming that the Lys8/Glu68 interaction contributes to the overall protein stability.

In the case of the wild-type HT, there is a difference in the T_m value of ~20 °C between the two redox forms; i.e., the T_m values of the oxidized and reduced forms are 109.8 and 129.7 °C, respectively (*21*) (Table 1). In the absence of a large difference in the structure between the oxidized and reduced proteins, the large difference in the stability between them should be due to the redox-dependent chemical nature of the heme active site. Generally, cationic ferriheme in an oxidized protein is less favorable in the hydrophobic environment of the heme pocket compared with neutral ferroheme in the reduced one (*33*−*37*). In addition, we also found a close relationship between the stabilities of the protein structure and the Fe−Met coordination bond (*14*, *17*). Therefore, the greater stability of the reduced protein than that of the oxidized one could also be due to the much greater Fe−Met bond stability in the former than the latter (*14*, *17*). The great stability of the Fe−Met bond in a reduced protein has been interpreted in terms of the conventional hard and soft acid and base principle, which dictates that relatively soft Fe^{2+} forms a more stable bond with the soft thioether sulfur atom of a Met side chain than hard Fe^{3+} does (*38*). Consequently, the stability of the Fe−Met bond in the oxidized protein is more greatly susceptible to alteration of the chemical environment due to mutations than that in the reduced one, because the former bond is weaker than the latter. As a result, the T_m value of the oxidized protein is usually more greatly affected by a given mutation than that of the reduced one. Upon removal of the Lys8/Glu68 interaction by the K8A mutation, the T_m values of the oxidized and reduced forms of the wild-type HT (Y25F mutant) were decreased by ~9 (~6) and ~6 (~2) degrees, respectively. Thus, as in the cases of the amino acid replacements in the hydrophobic protein interior such as the Y25F mutation, for a given protein, the T_m value of the oxidized form is more largely affected by the K8A mutation than that of the reduced one.

Furthermore, the removal of the Lys8/Glu68 interaction by the mutation is likely to lead to an enthalpically unfavorable contribution as well as an entropically favorable one to the protein stability. The enthalpic loss of the overall protein stability is simply due to removal of the intramolecular ionic pairing by the mutation. On the other hand, the entropic gain of the overall protein stability is expected to arise from an increase in the conformational freedom, together with a possible increase in the internal mobility, as a consequence of the removal of the interaction between the N- and C-terminal helices of the protein. The decreases in the thermostabilities of the proteins caused by the K8A mutation, as reflected in the T_m values (Table 1), indicated that the enthalpic loss prevails over the entropic gain.

Effects of the K8A Mutation on the E_m, ΔH, and ΔS Values. We next analyzed the effects of the K8A mutation on the E_m, ΔH, and ΔS values of the protein. We previously demonstrated through studies on HT and PA, and their mutant proteins, in which a series of amino acid residues in the protein interior were replaced, that the E_m value of a mutant protein showing higher stability in the oxidized form exhibits a negative shift relative to that of the wild-type protein in an enthalpic manner (*15*, *17*, *21*). Since the stability of the oxidized protein is more greatly affected by amino acid replacements in the hydrophobic protein interior than that of the reduced one, the E_m value is altered by the mutations through their effect on the difference in the thermodynamic stability between the oxidized and reduced forms. Hence, the redox function of a protein can be enthalpically controlled through the stability of the oxidized form by altering the contextual stereochemical packing of hydrophobic residues in the protein interior (*15*, *17*, *21*).

In contrast to the cases of the mutants previously studied (*17*, *21*), the E_m values of the K8A and K8A/Y25F mutants were decreased by ~8 and ~7 mV relative to those of the wild-type HT and Y25F mutant, respectively, although the stabilities of the oxidized proteins were decreased by the K8A mutation (Table 1). As can be seen in Table 1, the observed small, but subtle, decrease in the E_m value of the protein due to the K8A mutation was found to arise as a result of a competitive balance between the effects of the mutation on the ΔH and ΔS values.

Furthermore, comparison of the thermodynamic parameters among the proteins revealed that the $|\Delta H^{low}|$ and $|\Delta H^{high}|$ values of the K8A and K8A/Y25F mutants are larger than those of the corresponding counterpart proteins, i.e., the wild-type HT and Y25F mutant. This finding indicated that the enthalpic loss due to the removal of the intramolecular interaction by the K8A mutation is larger in the oxidized protein than the reduced one. In addition, the proteins rank wild-type HT (≈Y25F) < K8A < K8A/Y25F, in order of increasing $|\Delta S^{low}|$ and $|\Delta S^{high}|$ values (Table 1). The ΔS^{low} values of the wild-type HT (Y25F mutant) and the K8A and K8A/Y25F mutants are equivalent to -8.5 ± 0.6, -11.6 ± 0.6, and -14.2 ± 0.6 kJ mol^{-1}, respectively, at 25 °C. Hence the K8A mutation was found to decrease the ΔS values of the wild-type HT and Y25F mutant by 3.1 ± 0.6 and 5.7 ± 0.6 kJ mol^{-1}, respectively, at 25 °C. Thus, the effect of the K8A mutation on the entropy of the protein depends upon both the redox state and structure of the protein. Consequently, the K8A mutation is different from those in the hydrophobic protein interior such as the Y25F one in terms of the effect on the ΔS value, because the ΔS value was shown to be essentially independent of mutations in the protein interior (*15*, *17*, *21*). The K8A mutation-induced conformational change of the loop region bearing axial Met59, as suggested by the NMR structural comparison among the proteins, is possibly a structural factor responsible for the effect of the mutation on the ΔS value. It has been proposed that a redox-dependent solvent reorganization effect plays a significant role in the ΔS control of proteins (*39*−*41*). With the enhanced conformational freedom and internal mobility of the protein, as a result of the removal of the interaction contributing to stabilization of the association of two helices at opposite ends of the polypeptide chain, the solvent accessibility of the protein, and hence the redox-dependent solvent reorganization effect, is likely to be enhanced in the K8A mutants. In addition, since the internal mobility of a protein

has been shown to play a crucial role in ΔS control (*42*), the enhanced internal mobility in the K8A mutants is also expected to contribute to the effect of the mutation on the ΔS value.

CONCLUDING REMARKS

In order to determine the functional role of the highly conserved electrostatic interaction between the two helices at opposite ends of the polypeptide chain of cyts *c*, the protein stability and redox function of a mutant of HT, in which the interaction was abolished by amino acid replacement, have been characterized and compared with those of the wild-type HT. The comparison revealed that the thermodynamic properties of the protein are greatly affected by the amino acid replacements, demonstrating that the interaction plays a role in the control of the functional properties of the protein. Considering that the interaction occurs at 1.4 nm away from the heme iron and on the protein surface, the present results emphasize the importance of certain amino acid residues, relatively remote from the heme active site, in the functional control of the protein. This finding provides novel insights as to functional control of a protein, which could be utilized for tuning of the E_m value of the protein by means of protein engineering.

ACKNOWLEDGMENT

We thank Mr. Masato Kage for assistance in the preliminary NMR experiments. The ^{1}H NMR spectra were recorded on a Bruker Avance 600 spectrometer at the Chemical Analysis Center, University of Tsukuba.

SUPPORTING INFORMATION AVAILABLE

Superpositioning of ^{1}H−^{15}N HSQC spectra of the reduced forms of the ^{15}N uniformly labeled wild-type HT and K8A mutant in ∼90% ^1H_2O/∼10% ^2H_2O, pH 6.00, at 23 °C, temperature dependence of 600 MHz ^{1}H NMR spectra of the oxidized forms of the K8A and K8A/Y25F mutants at pH 7.0, temperature dependence of circular dichroism spectra of the oxidized and reduced forms of the K8A and K8A/Y25F mutants at pH 7.0, and pH profiles of the E_m values of the wild-type HT and K8A, Y25F, and K8A/Y25F mutants at 25 °C. This material is available free of charge via the Internet at http://pubs.acs.org.

REFERENCES

1. Zheng, Z., and Gunner, M. R. (2009) Analysis of the electrochemistry of hemes with E_ms spanning 800 mV. *Proteins 75*, 719–734.
2. Moore, G. R., and Pettigrew, G. W. (1990) Cytochromes c: Evolutionary, structural, and physicochemical aspects , Springer-Verlag, Berlin.
3. Scott, R. A., and Mauk, A. G., eds. (1996) Cytochrome c: A multidisciplinary approach , University Science Books, Sausalito, CA.
4. Warshel, A., Papazyan, A., and Muegge, I. (1997) Microscopic and semimacroscopic redox calculations: what can and cannot be learned from continuum models. *J. Biol. Inorg. Chem. 2*, 143–152.
5. Gunner, M. R., Alexov, E., Torres, E., and Lipovaca, S. (1997) The importance of the protein in controlling the electrochemistry of heme metalloproteins: Methods of calculation and analysis. *J. Biol. Inorg. Chem. 2*, 126–134.
6. Battistuzzi, G., Bellei, M., Borsari, M., Canters, G. W., de Waal, E., Jeuken, L. J., Ronieri, A., and Sola, M. (2003) Control of metalloprotein reduction potential: Compensation phenomena in the reduction thermodynamics of blue copper proteins. *Biochemistry 42*, 9214–9220.
7. Blouin, C., and Wallace, C. J. A. (2001) Protein matrix and dielectric effect in cytochrome *c*. *J. Biol. Chem. 276*, 28814–28818.
8. Springs, S. L., Bass, S. E., and McLendon, G. L. (2000) Cytochrome b_{562} variants: A library for examining redox potential evolution. *Biochemistry 39*, 6075–6082.
9. Travaglini-Allocatelli, C., Gianni, S., Dubey, V. K., Borgia, A., Di Matteo, A., Bonivento, D., Cutruzzola, F., Bren, K. L., and Brunori, M. (2005) An obligatory intermediate in the folding pathway of cytochrome c_{552} from *Hydrogenobacter thermophilus*. *J. Biol. Chem. 280*, 25729–25734.
10. Matsuura, Y., Takano, T., and Dickerson, R. E. (1982) Structure of cytochrome c_{551} from *Pseudomonas aeruginosa* refined at 1.6 Å resolution and comparison of the two redox forms. *J. Mol. Biol. 156*, 389–409.
11. Hasegawa, J., Shimahara, H., Mizutani, M., Uchiyama, S., Arai, H., Ishii, M., Kobayashi, Y., Ferguson, S. J., Sambongi, Y., and Igarashi, Y. (1999) Stabilization of *Pseudomonas aeruginosa* cytochrome c_{551} by systematic amino acid substitutions based on the structure of thermophilic *Hydrogenobacter thermophilus* cytochrome c_{552}. *J. Biol. Chem. 274*, 37533–37537.
12. Hasegawa, J., Uchiyama, S., Tanimoto, Y., Mizutani, M., Kobayashi, Y., Sambongi, Y., and Igarashi, Y. (2000) Selected mutations in a mesophilic cytochrome *c* confer the stability of a thermophilic counterpart. *J. Biol. Chem. 275*, 37824–37828.
13. Uchiyama, S., Hasegawa, J., Tanimoto, Y., Moriguchi, H., Mizutani, M., Igarashi, Y., Sambongi, Y., and Kobayashi, Y. (2002) Thermodynamic characterization of variants of mesophilic cytochrome *c* and its thermophilic counterpart. *Protein Eng. 15*, 455–461.
14. Yamamoto, Y., Terui, N., Tachiiri, N., Minakawa, K., Matsuo, H., Kameda, T., Hasegawa, J., Sambongi, Y., Uchiyama, S., Kobayashi, Y., and Yamamoto, Y. (2002) Influence of amino acid side chain packing on Fe-methionine coordination in thermostable cytochromes *c*. *J. Am. Chem. Soc. 124*, 11574–11575.
15. Terui, N., Tachiiri, N., Matsuo, H., Hasegawa, J., Uchiyama, S., Kobayashi, Y., Igarashi, Y., Sambongi, Y., and Yamamoto, Y. (2003) Relationship between redox function and protein stability of cytochromes *c*. *J. Am. Chem. Soc. 125*, 13650–13651.
16. Uchiyama, S., Ohshima, A., Nakamura, S., Hasegawa, J., Terui, N., Takayama, S. J., Yamamoto, Y., Sambongi, Y., and Kobayashi, Y. (2004) Complete thermal-unfolding profiles of oxidized and reduced cytochromes *c*. *J. Am. Chem. Soc. 126*, 14684–14685.
17. Takayama, S. J., Mikami, S., Terui, N., Mita, H., Hasegawa, J., Sambongi, Y., and Yamamoto, Y. (2005) Control of the redox potential of *Pseudomonas aeruginosa* cytochrome c_{551} through the Fe-Met coordination bond strength and pK_a of a buried heme propionic acid side-chain. *Biochemistry 44*, 5488–5494.
18. Mikami, S., Tai, H., and Yamamoto, Y. (2009) Effect of the redox-dependent ionization state of the heme propionic acid side chain on the entropic control of the redox potential of *Pseudomonas aeruginosa* cytochrome c_{551}. *Biochemistry 48*, 8062–8069.
19. Takayama, S. J., Irie, K., Tai, H., Kawahara, T., Hirota, S., Takabe, T., Alcaraz, L. A., Donaire, A., and Yamamoto, Y. (2009) Electron transfer from cytochrome *c* to cupredoxin. *J. Biol. Inorg. Chem. 14*, 821–828.
20. van den Burg, B., and Eijsink, V. G. H. (2002) Selection of mutations for increasing protein stability. *Curr. Opin. Biotechnol. 13*, 333–337.
21. Takahashi, Y., Sasaki, H., Takayama, S. J., Mikami, S., Kawano, S., Mita, H., Sambongi, Y., and Yamamoto, Y. (2006) Further enhancement of the thermostability of *Hydrogenobacter thermophilus* cytochrome c_{552}. *Biochemistry 45*, 11005–11011.
22. Travaglini-Allocatelli, C., Cutruzzola, F., Bigotti, M. G., Staniforth, R. A., and Brunori, M. (1999) Folding mechanism of *Pseudomonas aeruginosa* cytochrome c_{551}: Role of electrostatic interactions on the hydrophobic collapse and transition state properties. *J. Mol. Biol. 289*, 1459–1467.
23. Piotte, M., Saudek, V., and Sklená, V. (1992) Gradient-tailored excitation for single-quantum NMR spectroscopy of aqueous solutions. *J. Biol. NMR 2*, 661–665.
24. Lojou, E., and Bianco, P. (2000) Membrane electrodes can modulate the electrochemical response of redox potentials—Direct electrochemistry of cytochrome *c*. *J. Electroanal. Chem. 485*, 71–80.
25. Takayama, S. J., Takahashi, Y., Mikami, S., Irie, K., Kawano, S., Yamamoto, Y., Hemmi, H., Kitahara, R., Yokoyama, S., and Akasaka, K. (2007) Local conformational transition of *Hydrogenobactor thermophilus* cytochrome c_{552} relevant to its redox potential. *Biochemistry 46*, 9215–9224.
26. Yee, E. L., Cave, R. J., Guyer, K. L., Tyma, P. D., and Weaver, M. J. (1979) A survey of ligand effects upon the reaction entropies of some transition metal redox couples. *J. Am. Chem. Soc. 101*, 1131–1137.

27. Battistuzzi, G., Borsari, M., Loschi, L., Menziani, M. C., De Rienzo, F., and Sola, M. (2001) Control of metalloprotein reduction potential: The role of electrostatic and solvation effects probed on plastocyanin mutants. *Biochemistry 40*, 6422–6430.
28. La Mar, G. N., Satterlee, J. D., and de Ropp, J. S. (2000) Nuclear magnetic resonance of hemoproteins, in The porphyrin handbook (Kadish, K., Smith, K. M., and Guilard, R., Eds.) pp 185−298, Academic Press, New York.
29. Bertini, I., and Luchinat, C. (1986) NMR of paramagnetic molecules in biological systems , pp 19−46, Benjamin/Cummings Publishing Co., Menlo Park, CA.
30. Yamamoto, Y. (1998) NMR study of active sites in paramagnetic hemoproteins. *Annu. Rep. NMR Spectrosc. 36*, 1–77.
31. Kay, L. E., Keifer, P., and Saarinen, T. (1992) Pure absorption gradient enhanced heteronuclear single quantum correlation spectroscopy with improved sensitivity. *J. Am. Chem. Soc. 114*, 10663–10665.
32. Takahashi, Y., Takayama, S. J., Mikami, S., Mita, H., Sambongi, Y., and Yamamoto, Y. (2006) Influence of a single amide group on the redox function of *Pseudomonas aeruginosa* cytochrome c_{551}. *Chem. Lett. 35*, 528–529.
33. Komar-Panicucci, S., Weis, D., Bakker, G., Qiao, T., Sherman, F., and McLendon, G. (1994) Thermodynamics of the equilibrium unfolding of oxidized and reduced *Saccharomyces cerevisiae* Iso-1-cytochromes c. *Biochemistry 33*, 10556–10560.
34. Battistuzzi, G., Borsari, M., Sola, M., and Francia, F. (1997) Redox thermodynamics of the native and alkaline forms of eukaryotic and bacterial class I cytochromes *c*. *Biochemistry 36*, 16247–16258.
35. Tezcan, F. A., Winkler, J. R., and Gray, H. B. (1998) Effects of ligation and folding on reduction potentials of heme proteins. *J. Am. Chem. Soc. 120*, 13383–13388.
36. Battistuzzi, G., Borsari, M., and Sola, M. (2001) Medium and temperature effects on the redox chemistry of cytochrome *c*. *Eur. J. Inorg. Chem. 2001*, 2989–3004.
37. Battistuzzi, G., Borsari, M., Ranieri, A., and Sola, M. (2002) Redox thermodynamics of the Fe^{3+}/Fe^{2+} couple in horseradish peroxidase and its cyanide complex. *J. Am. Chem. Soc. 124*, 26–27.
38. Rovira, C., Carloni, P., and Parrinello, M. (1999) The iron-sulfur bond in cytochrome *c*. *J. Phys. Chem. B 103*, 7031–7035.
39. Battistuzzi, G., Borsari, M., Ronieri, A., and Sola, M. (2004) Solvent-based deuterium isotope effects on the redox thermodynamics of cytochrome *c*. *J. Biol. Inorg. Chem. 9*, 781–781.
40. Battistuzzi, G., Borsari, M., Ronieri, A., and Sola, M. (2002) Redox thermodynamics of the Fe^{3+}/Fe^{2+} couple in horseradish peroxidase and its cyanide complex. *J. Am. Chem. Soc. 124*, 26–27.
41. Sola, M, Battistuzzi, G., and Borsari, M. (2005) Modulation of the free energy of reduction in metalloproteins. *Chemtracts: Inorg. Chem. 18*, 73–86.
42. Banci, L., Bertini, I., Huber, J. G., Spyroulias, G. A., and Turano, P. (1999) Solution structure of reduced horse heart cytochrome *c*. *J. Biol. Inorg. Chem. 4*, 21–31.